Scientia Iranica (2024) 31(10), 790–797

Sharif University of Technology
Scientia Iranica
Transactions D: Computer Science & Engineering and Electrical Engineering
https://scientiairanica.sharif.edu

Performance improvement of the hybrid switch reluctance motor by notching method

S. Hasanzadeh[a,*], H. Rezaei[b], and H. Taheri[a]

a. *Department of Electrical and Computer Engineering, Qom University of Technology, Qom, Iran.*
b. *Department of Electrical and Computer Engineering, Babol Noshirvani University of Technology, Babol, Iran & Mazandaran Regional Electric Company, Sari, Iran.*

Received 4 November 2021; received in revised form 12 February 2022; accepted 9 May 2022

KEYWORDS
Hybrid Switch Reluctance Motor (HSRM);
Finite Element Method (FEM);
Ripple torque;
Average torque;
Notching.

Abstract. Hybrid switch reluctance motors belong to the family of Switch Reluctance Motors (SRMs) that attenuate magnetic saturation and increase air gap magnetic flux by exploiting permanent magnets. The auxiliary air gap flux generated by permanent magnets can affect the average torque and ripple. Typically, reducing torque ripple results in a decrease in average torque. This paper focuses on reducing torque ripple and enhancing average torque in a 6/10 pole hybrid switch reluctance motor by inserting two symmetrical notches on its rotor. Also, the lengths of the magnet and rectangular notches are optimized using the finite element method and sensitivity analysis. A comparison between the optimized design and the initial one, conducted through finite element analysis, proves the efficiency of the proposed model.

1. Introduction

The simple structure, fault tolerance, reliability, and robustness due to the absence of winding structure in the rotor of Switch Reluctance Motors (SRMs) have attracted particular attention in domestic applications [1–3]. Also, Hybrid Switch Reluctance Motors (HSRMs), using Permanent Magnets (PMs), can develop higher average torque and better starting capability with less-saturated core operation [4,5]. However, the high torque ripple is considered a major drawback that limits its applications.

Increasing the number of rotor poles in [5] leads to a higher starting torque, lower high-speed torque, and better torque ripple. Also, the saturation performance, average, and starting torques are improved by adding PMs to SRM. In [6], the laminated stator and rotor topology is proposed to improve average torque and torque ripple using short-flux magnetic paths. However, this design causes the core product to be complicated. The stator tooth angle, rotor pole arc, and PM thickness are optimized for better torque development and load capability using Finite Element Method (FEM) in the modular-stator HSRM [7,8]. In

*. *Corresponding author.*
E-mail addresses: hasanzadeh@qut.ac.ir (S. Hasanzadeh); hosseinrezaei1367@nit.ac.ir (H. Rezaei); hadistaheri1997@gmail.com (H. Taheri)

To cite this article:
S. Hasanzadeh, H. Rezaei, and H. Taheri "Performance improvement of the hybrid switch reluctance motor by notching method", *Scientia Iranica* (2024) **31**(10), pp. 790-797
DOI: 10.24200/sci.2022.59347.6190

[9], a Genetic Algorithm (GA) is utilized to optimize the dimensions of rotor tooth, stator yoke, and stator window for maximum average torque and minimum torque ripple. An objective function focusing on high starting torque, low torque ripple, and high efficiency are proposed in [10] to optimize the rotor and stator pole arcs and outer rotor diameter of an HSRM using FEM. Although in some research, SRM torque ripple is considered an objective in optimization, it remains unresolved and still high, posing a challenge. In [11], torque ripple is decreased significantly through notching the rotor structure, which strongly impacts the flux harmonics and torque ripple minimization. However, the average torque is also weakened by inserting a single notch into the rotor structure. A notching method is a practical approach implemented on the rotor/stator topology to reduce torque ripple, noise, and power factor [12,13]. Despite its simplicity and effectiveness in improving several performance indices, this approach is not given full attention in most papers dealing with HSRM design and optimization. The reduction of developed torque is another challenge in the notching method. The method presented in this paper can be developed and implemented on linear machines with similar hybrid structures [14,15].

In this paper, the structure of an HSRM is improved by adding two symmetrical notches on the rotor. Subsequently, the PM length and notching span are optimized using FEM to improve the average torque in a minimum PM length and torque ripple. The organization of this paper is as follows: In Section 2, the initial design and topology of HSRM are described. Section 3 deals with the principles and parameters of the design and methods of reducing the proposed motor ripple, such as the longitudinal dimensions of the magnet. Section 4 presents the simulation results. Section 5 describes the design of the new rotor structure for the proposed motor, and the final conclusions are made in Section 6.

2. Permanent magnet-reinforced HSRM

The HSRM topology is depicted in Figure 1. The initial design parameters of the hybrid reluctance switch motor are selected based on Ref. [9] and listed in Table 1. The initial design consists of 6 stator poles and 10 rotor poles with PMs adjusted adjacent to the stator pole. The operation of the HSRM is based on the use of a PM. The function of the magnets attenuates the magnetic saturation at the stator pole and increases the magnetic flux in the air gap, which can significantly increase the output torque. The HSRM magnetic equivalent circuit is symmetrical, and the magnetic excitation magnetomotive force (MMF) is provided by the magnet and the field current in each phase. The operation of the magnetic core at the knee point of the B-H curve causes the nonlinear behavior of the HSRMs, creating harmonics and torque ripple, consequently.

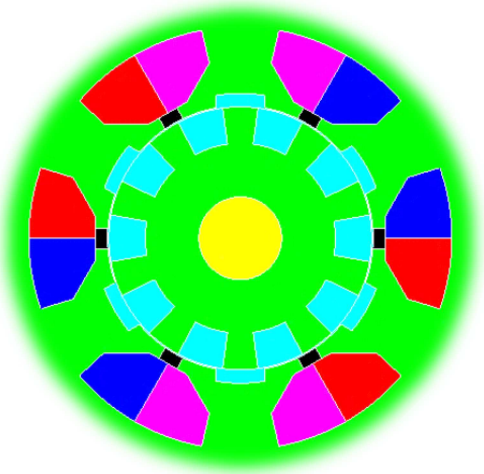

Figure 1. The initial design of HSRM.

Table 1. Design parameters of HSRM.

Outer diameter of the stator (mm)	120
Air gap (mm)	0.3
Phase	3
Number of coils	140
PM thickness (mm)	3
Rotor diameter (mm)	63.7
Power (Watts)	770
Speed (rpm)	1000

3. Optimized design

In this section, the design improvement and optimization are carried out to mitigate the torque performance. As such, two symmetrical notches are inserted on the rotor. To evaluate the ripple performance and average torque, the impact of PM length and notch dimensions is analyzed using FEM sensitivity analysis. Figure 2 shows a modified design achieved by creating notches in rotor poles using the notching method.

3.1. Notch creation on the rotor

In HSRMs, magnetic torque is produced by the interaction of rotor parts and stator teeth. The internal gravitational force between the teeth and the motor poles tries to maintain a balance between the stator teeth and rotor sections; to reduce this equilibrium, it is necessary to minimize the effect of harmonic flux changes on the air gap.

Creating symmetrical, small, and smooth notches at the end of rotor poles reduces the harmonic distortion of the air-gap flux and torque ripple. However, the developed torque is also decreased due to an increase

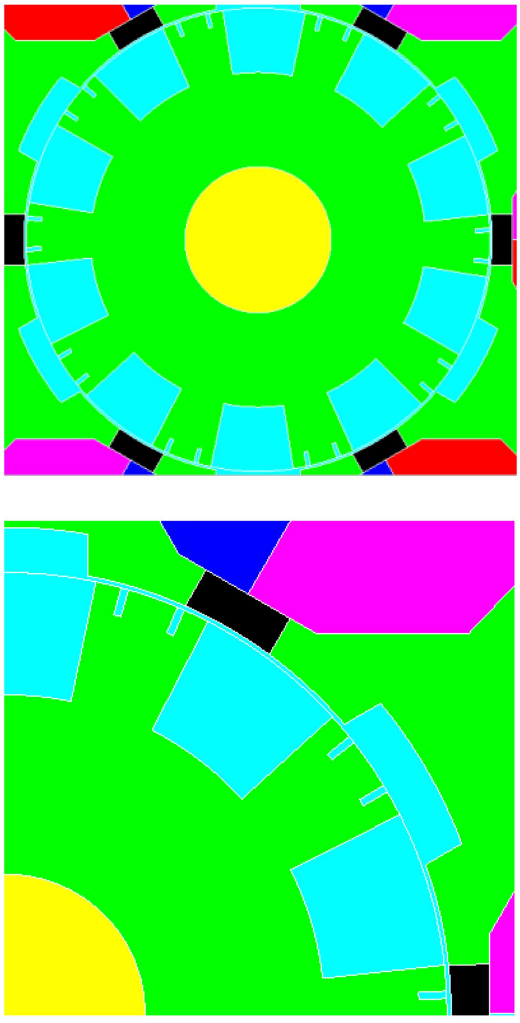

Figure 2. A modified design by creating notches in rotor pole with notching method.

Figure 3. Notch design model and parameter.

in the effective air gap and flux weakening. Therefore, the average torque should be observed in addition to investigating the impact of notches on torque ripple. To achieve this balance, the notch height and number should be carefully selected. In this study, two symmetrical notches with a height of 2 mm are inserted at each rotor pole. Structures with more than two notches and 2 mm height cause a significant reduction in average torque. Also, the optimum notching span will be found via sensitivity analysis. According to Figure 3, two rectangular notches are inserted symmetrically at the end of rotor poles to reduce air-gap flux and torque ripple harmonics. The notching span α_n can be derived as a function of the notching height h_n, efficiency η, and rotor radius R_1:

$$\alpha_n = \eta \frac{h_n}{R_1}. \tag{1}$$

In the proposed model, the notching span α_n varies between 0 and 1 with a step of 0.1, and the notching height h_n is fixed at 2 mm. The harmonic distortion of the air-gap flux is managed by selecting the appropriate notching span value, which reduces torque ripple.

However, like other common methods for torque ripple reduction, the notching method reduces torque ripple and average torque, which is not optimal. Therefore, it is necessary to check the magnetic part to compensate for the average torque reduction. For this purpose, the optimum PM length can be selected by considering the torque ripple, average torque, and PM cost.

3.2. The effect of PM length on average torque

Like electromagnet coils, PMs create a MMF proportional to their length and magnetization (magnetization length), through which the generated magnetic flux passes through various air paths. Consequently, the flux density increases with the magnetization length. However, as the length of magnetization increases, the PM flux weakens as it closes in longer air gap paths, reducing the developed torque. Therefore, an excessive increase in PM magnetization length can deteriorate torque performance. As depicted in Figure 4 and Table 2, in the rotor structure without notches, increasing the PM length significantly reduces torque ripple, but it does not necessarily increase the average torque. Therefore, there exists an optim PM length for each rotor structure. The following section evaluates torque performance in different notching

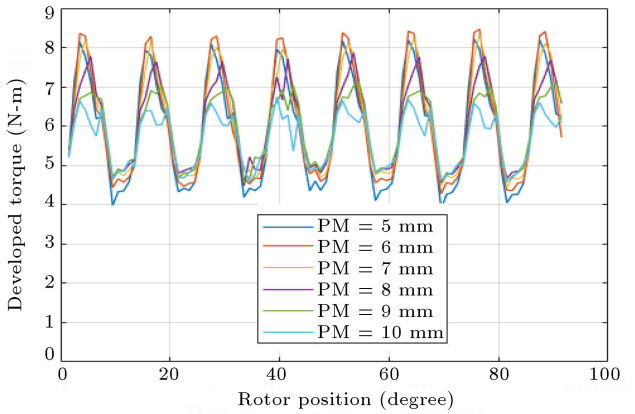

Figure 4. Developed torque vs. rotor position in various PM lengths for notchless rotor structure.

Table 2. Average torque and torque ripple vs. PM length in notchless rotor structure.

PM length (NdeFeB)	Average torque (N-m)	Variation of T_{ave} decrease (−) increase (+)	Torque ripple (%)	Variation of ripple decrease (−) increase (+)
PM = 5 mm	5.95	0%	72.62	0%
PM = 6 mm	6.1004	+2.48%	68.69	−5.41%
PM = 7 mm	6.142	+3.18%	63.6	−12.41%
PM = 8 mm	6.082	+2.178%	55.69	−23.31%
PM = 9 mm	5.935	−0.296%	43.29	−40.74%
PM = 10 mm	5.661	−4.89%	38.15	−47.46%

Table 3. Motor models with different PM lengths and notching spans.

Model	PM length (mm)	Notching span	Notching height (mm)
I1	5	Range 0 to 1 with a ratio of 0.1	2
I2	6	Range 0 to 1 with a ratio of 0.1	2
I3	7	Range 0 to 1 with a ratio of 0.1	2
I4	8	Range 0 to 1 with a ratio of 0.1	2
I5	9	Range 0 to 1 with a ratio of 0.1	2
I6	10	Range 0 to 1 with a ratio of 0.1	2

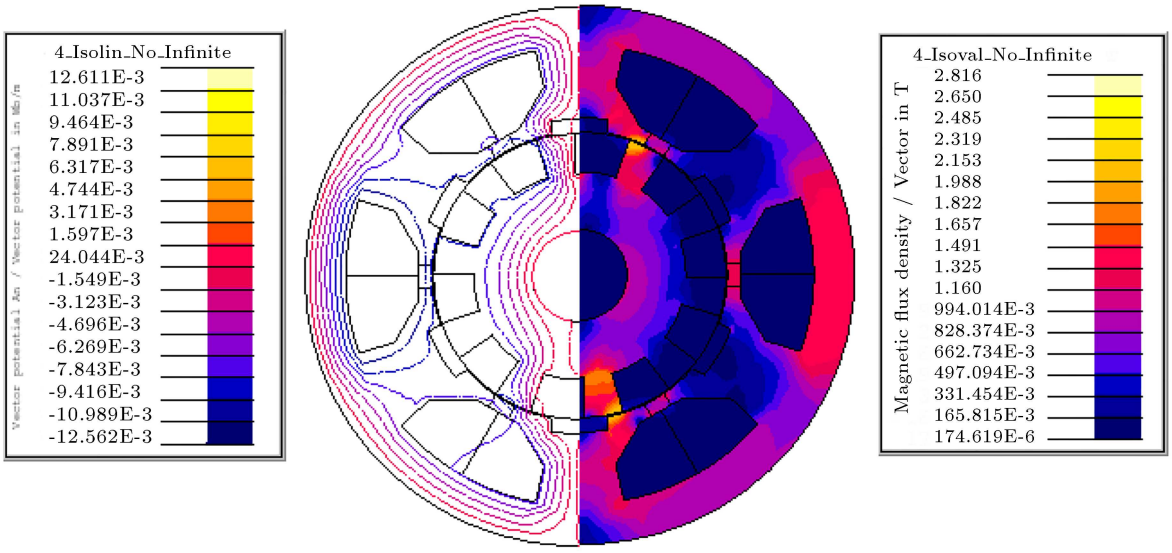

Figure 5. Flux lines and flux density spectrum.

spans and PM lengths using FEM. As listed in Table 3, the PM length varies between 5 to 10 mm in models I1 to I6. In each model, the notching span varies from 0 to 1 in increments of 0.1, while the notching height remains constant. As a result, the optimum PM length and notching span can be derived. The developed torque versus PM length is illustrated in Figure 4. Also, the average torque, torque ripple, and variations percentage compared to the initial design are also presented in Table 2.

4. Simulation results

In this section, the HSRM performance is analyzed to evaluate and compare torque ripple and average torque in different magnet lengths and notching spans at a rotational speed of 1000 rpm and a field current of 20 amperes with FEM simulations. Additionally, the flux lines and their spectrum are depicted in Figure 5. The specifications of the finite element model are listed in Table 4.

Table 4. Finite element specifications.

Timestep	0 to 0.015 (1.67e-4 sec)
Solution type	Transient
Mesh information	14549 nodes 1523 line elements 7244 surface elements

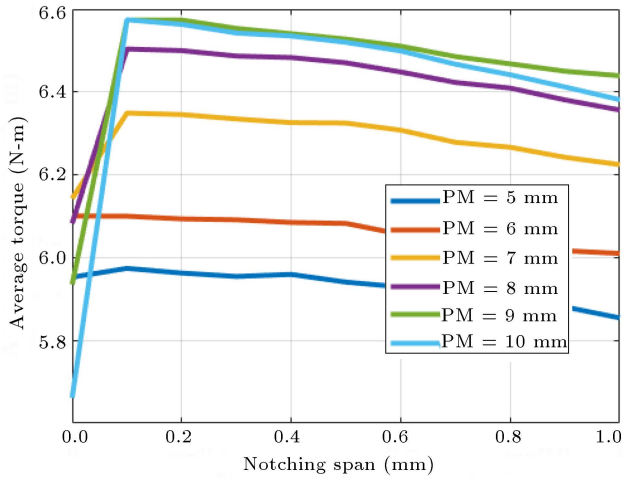

Figure 6. Variations of average torque versus notching span in various PM lengths.

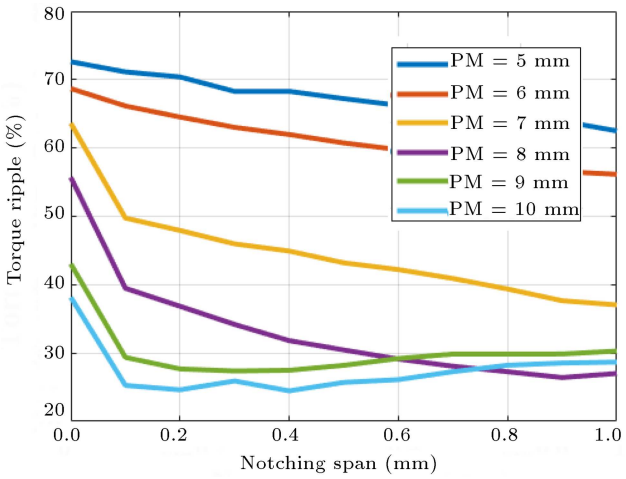

Figure 7. Variations of torque ripple versus notching span in various PM lengths.

This sensitivity analysis aims to find the appropriate rotor notch and PM length values to achieve minimal torque ripple while maintaining acceptable average torque. As stated in the previous section, six different modes are designed, applied, and simulated on the initial design. The variations of average torque and torque ripple are derived through FEM across different notching spans and PM lengths, as illustrated in Figures 6 and 7. In model I1, the PM length is 5 mm, and notching span varies between 0 to 1 mm with a ratio of 0.1. According to Figures 6 and 7, the torque ripple and average torque decrease in the same way. However, the torque ripple intensifies when the notching span varies from 0.1 to 0.2 mm.

The results show that compared to the initial model, torque ripple and average torque are reduced up to 13.9% and 1.6%, respectively. Notably, a larger notching span leads to a more significant impact on ripple reduction. In Model I2, the magnet length was 6 mm. Increasing the magnet length positively affects the improvement of the objectives of average torque and ripple. As seen in Figures 6 and 7, increasing the PM length does not necessarily strengthen the average torque. Particularly, between 9 to 10 mm PM length, the average torque weakens in all notching spans. Although increasing the PM length strengthens the magnetic flux and developed torque due to magnetic MMF amplification, magnetic reluctance is increased at higher PM lengths. This, in turn, attenuates the flux field and output torque. Therefore, while PM length always reduces torque ripple, it does not always increase average torque.

5. Optimum designs of HSRM

This paper defines the objective function based on achieving maximum average torque, minimum torque ripple, and considering the PM cost by incorporating PM length into the function. The objective function is defined as:

$$\text{Cost} - Function = \left(a \times T_{ave} + b \times Ripple\right) \frac{PM\_Length}{100}, \quad (2)$$

where T_{ave} is the average torque, the coefficient "a" should be negative to minimize the cost function, whereas the coefficient "b" has a positive value. These coefficients are selected depending on the designer's emphasis. The design variables are PM length and notch dimensions. In Eq. (2), other design parameters such as air gap and PM thickness are assumed to be constant. The definition of the cost function is entirely a matter of preference, and we define it to emphasize the main goal, which is to increase the average torque and decrease the ripple at minimum PM cost.

This function shows that the lower the torque ripple and the higher the average torque, the smaller the numerical value of the target function in a defined and limited PM length. The optimum designs yielding minimum cost functions are attained, as shown in Figure 8. As written in Table 5, in addition to torque performance, the back-emf total harmonic distortion (back-emf THD) and power factor are improved in the optimum designs. Although the HSRM material cost

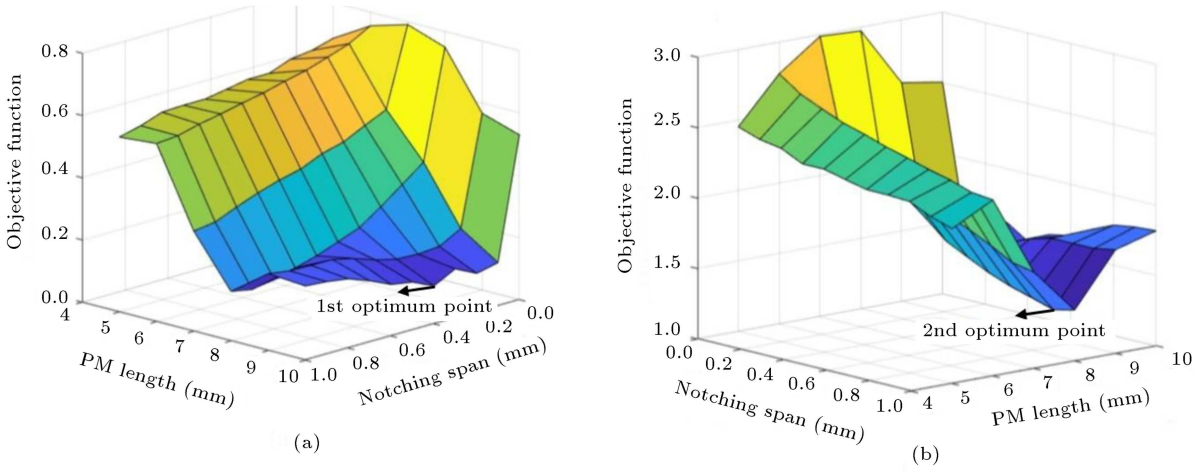

Figure 8. (a) First and (b) Second optimum designs of HSRM (PM length and notching span).

Table 5. Optimum designs of HSRM (PM length and notching span).

	PM length	Span	T_{ave} (N-m)	Ripple (%)	Back-emf THD (%)	PF (%)	Factors
Initial design	5 mm	0	5.95	72.6	56.6	0.413	–
1st optimal design	10 mm	0.4	6.54 (+9.8%)	24.5% (−66.3%)	52.9 (−6.5%)	0.439 (+6.3%)	$a = -0.75$ $b = 0.25$
2nd optimal design	8 mm	0.9	6.38 (+7.2%)	26.4% (−63.6%)	53.5 (−5.4%)	0.438 (+6.1%)	$a = -0.3$ $b = 0.7$
Experimental results in [9]	5 mm	0	7.3	68.5%	–	–	–

increases with the PM length in the optimum designs, a remarkable improvement in the torque ripple and average torque makes them financially reasonable.

The first optimum design is calculated with an emphasis on the average torque $(-0.25, 0.75)$. It is shown that there is a 9.77% improvement in average torque and a 66.3% improvement in torque ripple. Additionally, there is a 6.5% improvement in THD and a 6.3% improvement in PF compared to the initial state. Comparisons of developed torque in the optimum designs with the initial notchless topology are illustrated in Figure 9. Due to improvements in average torque, torque ripple, THD, and PF, this motor is significantly optimized. By selecting the weighting factors as $(-0.3, 0.7)$ in the cost function (2), the second optimum design is obtained with a magnet length of 8 mm and a notching span of 0.9 mm. In this design, a 63.6% reduction in torque ripple and a 7.2% increase in average torque have occurred. Improvements in THD and PF are also achieved, reaching 5.4% and 6.05%, respectively.

Table 5 shows that although the second design has less improvement than the first design in average torque and ripple, a 20% reduction in PM consumption is observed. Since its performance is close to the first design, this optimum point can be a desirable alternative for low-cost applications. Also, in Table 5, the optimum designs may be compared with the experimental results obtained in [9]. As can be observed, the experimental set-up in [9] offers better average torque despite severe torque ripple. The first optimum point reaches 89.5% of T_{ave} in [9] and a 64% improvement in torque ripple is achieved by consuming

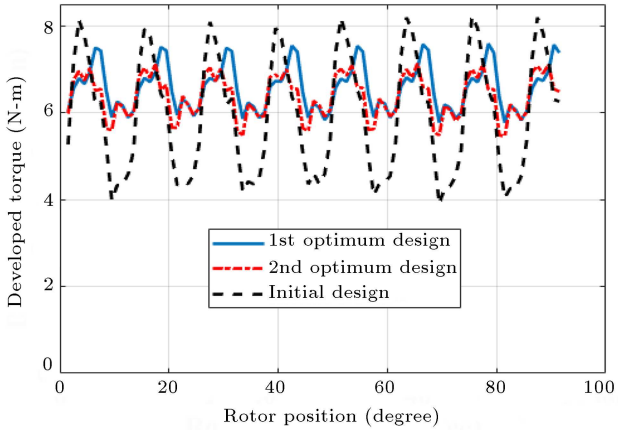

Figure 9. Developed torque vs. rotor position in initial and optimum designs.

100% more magnets. The average torque reaches 87.4% of T_{ave} in [9] for the second optimum design, with a 61.5% reduction in torque ripple with 60% more PM consumption compared to [9].

6. Conclusion

In this paper, optimum designs of a 6/10 pole hybrid switch reluctance motor are presented, optimizing the notching span of the rotor and Permanent Magnet (PM) length to improve performance. Different notching spans and PM lengths were investigated. Finally, two optimum designs were obtained based on the cost function, satisfying torque ripple and average torque while minimizing additional PM cost. The proposed model with a notching span of 0.4 mm and a PM length of 10 mm has been selected as the first optimum design. Compared to the notchless initial model, the torque ripple is improved by 66.3%, while the average torque is enhanced by 9.8%. In the second design, with more emphasis on torque ripple, these improvements are 63.6% and 7.2% respectively, while saving 20% in PM cost. Also, the proposed optimum designs decrease harmonic distortion and strengthen the power factor.

References

1. Bartolo, J.B., Degano, M., Espina, J., et al. "Design and initial testing of a high-speed 45-kW switched reluctance drive for aerospace application", *IEEE Trans. Ind. Electron.*, **64**(2), pp. 988–997 (2017). DOI: 10.1109/TIE.2016.2618342

2. Bostanci, E., Moallem, M., Parsapour, A., et al. "Opportunities and challenges of switched reluctance motor drives for electric propulsion: A comparative study", *IEEE Trans. Transp. Electrif.*, **3**(1), pp. 58–75 (2017). DOI: 10.1109/TTE.2017.2649883.

3. Naseh, M., Hasanzadeh, S., Dehghan, S.M., et al. "Optimized design of rotor barriers in pm-assisted synchronous reluctance machines with taguchi method", *IEEE Access*, **10**, pp. 38165–38173 (2022). DOI: 10.1109/ACCESS.2022.3165549

4. Ding, W., Hu, Y., Wang, T., et al. "Comprehensive research of modular E-core stator hybrid-flux switched reluctance motors with segmented and nonsegmented rotors", *IEEE Trans. Energy Convers.*, **32**(1), pp. 382–393 (2017). DOI: 10.1109/TEC.2016.2631248

5. Ding, W., Yang, S., and Hu, Y. "Development and investigation on segmented-stator hybrid-excitation switched reluctance machines with different rotor pole numbers", *IEEE Trans. Ind. Electron.*, **65**(5), pp. 3784–3794 (2018). DOI: 10.1109/TIE.2017.2760846

6. Ding, W., Yang, S., Hu, Y., et al. "Design consideration and evaluation of a 12/8 high-torque modular-stator hybrid excitation switched reluctance machine for EV applications", *IEEE Trans. Ind. Electron.*, **64**(12), pp. 9221–9232 (2017). DOI: 10.1109/TIE.2017.2711574

7. Shirali, E., Hasanzadeh, S., and Dehghan, S.M. "FEM-aided analytical model and control of SSLFSM thrust force", *Comput. Intell. Electr. Eng.*, **11**(2), pp. 87–94 (2020). DOI: 10.22108/ISEE.2019.114726.1189

8. Mousavi-Aghdam, S.R., Feyzi, M.R., Bianchi, N., et al. "Design and analysis of a novel high-torque stator-segmented SRM", *IEEE Trans. Ind. Electron.*, **63**(3), pp. 1458–1466 (2016). DOI: 10.1109/TIE.2015.2494531

9. Zhu, J., Cheng, K.W.E., and Xue, X. "Design and analysis of a new enhanced torque hybrid switched reluctance motor", *IEEE Trans. Energy Convers.*, **33**(33), pp. 1965–1977 (2018). DOI: 10.1109/TEC.2018.2876306

10. Diao, K., Sun, X., Lei, G., et al. "Multimode optimization of switched reluctance machines in hybrid electric vehicles", *IEEE Trans. Energy Convers.*, **36**, pp. 2217–2226 (2021). DOI: 10.1109/TEC.2020.3046721

11. Mehta, S., Kabir, M.A., Pramod, P., et al. "Segmented rotor mutually coupled switched reluctance machine for low torque ripple applications", *IEEE Trans. Ind. Appl.*, **57**(4), pp. 3582–3594 (2021). DOI: 10.1109/TIA.2021.3073384

12. Xiang, Z., Quan, L., and Zhu, X. "A new partitioned-rotor flux-switching permanent magnet motor with high torque density and improved magnet utilization", *IEEE Trans. Appl. Supercond.*, **26**(4), pp. 1–5 (2016). DOI: 0.1109/TASC.2016.2514486

13. Sikder, C., Husain, I., and Ouyang, W. "Cogging torque reduction in flux-switching permanent-magnet machines by rotor pole shaping", *IEEE Trans. Ind. Appl.*, **51**(5), pp. 3609–3619 (2015). DOI: 10.1109/TIA.2015.2416238

14. Esfahanian, H.R., Hasanzadeh, S., Heydari, M., et al. "Design, optimization, and control of a linear tubular machine integrated with levitation and guidance for maglev applications", *Sci. Iran.*, **30**(4), pp. 1330–1341 (2023). DOI: 10.24200/SCI.2021.57416.5231

15. Hasanzadeh, S., Rezaei, H., and Qiyassi, E. "Analysis and optimization of permanent magnet dimensions in electrodynamic suspension systems", *J. Electr. Eng. Technol.*, **13**(1), pp. 307–314 (2018). DOI: 10.5370/JEET.2018.13.1.307

Biographies

Saeed Hasanzadeh received his MSc and PhD degrees in electrical engineering from the University of Tehran (UT), Tehran, Iran, in 2006 and 2012, respectively. His MSc thesis and PhD dissertation focused on high voltage engineering and Wireless Power Transfer (WPT), respectively. In 2013, he joined the Department of Electrical and Computer Engineering at Qom University of Technology as an Assistant Professor. He was recognized as an Outstanding Lecturer at

Qom University of Technology in 2020 and currently serves as the Dean of the Department of Electrical and Computer Engineering (ECE). His research interests include power electronics, electrical machines, wireless power transfer, and high-voltage engineering. He is a TPC Member of the IEEE Power Electronics & Drives: Systems and Technologies Conference (PEDSTC). He was a recipient of the Top Research Prize of the Qom University of Technology in 2019. He also serves on the Editorial Board of the Power Electronics Society of Iran (PELSI).

Hossein Rezaei received his BS degree in electrical engineering from Shahid Beheshti University, Tehran, Iran, in 2011, and his MSc degree in electrical engineering from the University of Tehran, Iran, in 2013. He is currently pursuing his PhD degree in electrical engineering at Babol Noshirvani University of Technology, Iran. His research interests include hybrid and electrical vehicles, electrical machines, and power electronics.

Hadis Taheri received her BS degree in electrical engineering from Buein Zahra Technical University, Buein Zahra, Iran, in 2019, and her MSc degree in electrical engineering from Qom University of Technology, Qom, in 2021. Her research interests include power electronics and electrical machines.